

## Methylaminated Potassium Fulleride, $(\text{CH}_3\text{NH}_2)\text{K}_3\text{C}_{60}$ : Towards Hyperexpanded Fulleride Lattices

Alexey Yu. Ganin,<sup>†</sup> Yasuhiro Takabayashi,<sup>‡</sup> Craig A. Bridges,<sup>†</sup> Yaroslav Z. Khimyak,<sup>†</sup>  
Serena Margadonna,<sup>§</sup> Kosmas Prassides,<sup>\*,‡</sup> and Matthew J. Rosseinsky<sup>\*,†</sup>

Department of Chemistry, University of Liverpool, Liverpool L69 7ZD, U.K., Department of Chemistry, University of Durham, Durham DH1 3LE, U.K., and School of Chemistry, University of Edinburgh, Edinburgh EH9 3 JJ, U.K.

Received August 30, 2006; E-mail: k.prassides@durham.ac.uk; m.j.rosseinsky@liverpool.ac.uk

The electronic properties of metal fullerides are controlled by interfullerene separation and relative orientation. The most effective chemical means of controlling these parameters is the coordination of the ammonia molecule to the alkali metal cations,<sup>1</sup> resulting in a range of structures related to simple sphere packings that maintain electronic contact between the fulleride anions at a level sufficient to position the materials near the metal–superconductor–insulator boundary. It is therefore important to explore the chemistry of alkyl amines with fullerides. Surprisingly, methylamine has served only as a solvent for preparation of  $\text{A}_3\text{C}_{60}$  ( $\text{A} = \text{K}, \text{Rb}$ ) fullerides.<sup>2</sup> Here we report the intercalation of large neutral methylamine molecules into the fulleride lattice, opening the way to increasing the interfullerene separation beyond that achieved previously in ammoniated alkali fullerides.

Reaction of  $\text{K}_3\text{C}_{60}$  with methylamine (predried by distillation off K metal) vapor at  $\sim 3.5$  atm pressure (40 min, 23 °C) afforded a black, solid product whose composition was established by chemical analysis as  $(\text{CH}_3\text{NH}_2)_{1.00(7)}\text{K}_3\text{C}_{60}$ .<sup>3</sup> Raman spectroscopy at room temperature showed the presence of the  $\text{C}_{60} \text{A}_g(2)$  mode at  $1448(1) \text{ cm}^{-1}$  (Figure 1 inset), consistent with an unchanged charge of  $-3$  for the  $\text{C}_{60}$  units.<sup>4</sup> The solid-state MAS (20 kHz)  $^{13}\text{C}$  NMR spectrum of the material at room temperature (Figure 1) also exhibited a single sharp peak at 195.5 ppm attributable to the  $\text{C}_{60}^{3-}$  ions. Complementary fast (30 kHz) MAS  $^1\text{H}$  NMR measurements confirmed the co-intercalation of  $\text{CH}_3\text{NH}_2$  in the fulleride salt (Figure S1). They showed the presence of a sharp resonance at 5.5 ppm, attributed to the  $-\text{NH}_2$  protons and shifted downfield relative to that in uncoordinated  $\text{CH}_3\text{NH}_2$  (3.9 ppm),<sup>5</sup> consistent with the expected coordinative bonding to  $\text{K}^+$  ions. Further resonances are also present at 3.4, 2.8, and 0.5 ppm and are attributed to the  $-\text{CH}_3$  protons. Their considerably increased linewidths imply strongly restricted rotation of the methyl protons compared with those bound to nitrogen.

The high-resolution synchrotron X-ray powder diffraction pattern of  $(\text{CH}_3\text{NH}_2)\text{K}_3\text{C}_{60}$  is indexable with the face-centered orthorhombic (space group  $Fmmm$ ) unit cell of the ammonia analogue,  $(\text{NH}_3)\text{K}_3\text{C}_{60}$ .<sup>6</sup> Analysis with the LeBail technique resulted in lattice parameters,  $a = 15.205 \text{ \AA}$ ,  $b = 15.179 \text{ \AA}$ ,  $c = 13.503 \text{ \AA}$ , revealing a large change in the unit cell metrics. A notable feature of this result is that the  $(\text{CH}_3\text{NH}_2)\text{K}_3\text{C}_{60}$  structure is strongly anisotropic with four closest center-to-center  $\text{C}_{60}$  contacts of  $10.742 \text{ \AA}$  in the  $ab$  basal plane and eight of  $10.158$ – $10.167 \text{ \AA}$  perpendicular to it. While the latter contact is comparable to that in  $\text{K}_3\text{C}_{60}$  ( $\sim 10.1 \text{ \AA}$ ), the basal plane is largely expanded, giving rise to an overall volume inflation of  $\sim 7\%$  upon  $\text{CH}_3\text{NH}_2$  intercalation of  $\text{K}_3\text{C}_{60}$ . This is reminiscent of the situation encountered in  $(\text{NH}_3)\text{K}_3\text{C}_{60}$  where two dif-

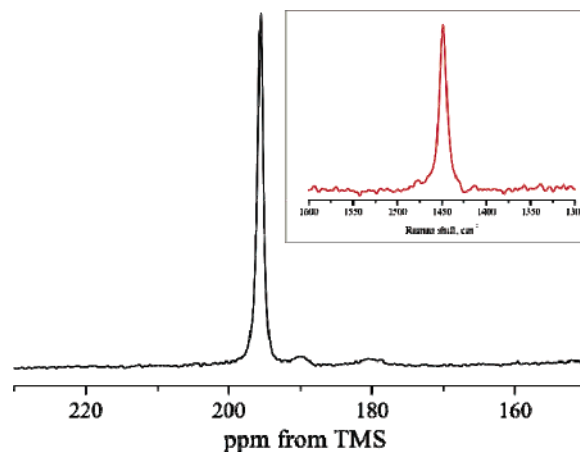


**Figure 1.** Solid-state MAS (20 kHz)  $^{13}\text{C}$  NMR spectrum of  $(\text{CH}_3\text{NH}_2)\text{K}_3\text{C}_{60}$  at ambient temperature. (Inset) Selected region of the Raman spectrum in the vicinity of the  $\text{C}_{60} \text{A}_g(2)$  mode.

ferent sets of  $\text{C}_{60}$ – $\text{C}_{60}$  contacts were also present ( $10.56 \text{ \AA}$  and  $10.11$ – $10.14 \text{ \AA}$ , respectively) and implies that  $\text{K}^+ - \text{NH}_2 - \text{CH}_3$  units reside in the large pseudo-octahedral voids of the parent cubic fulleride structure. Very importantly, the larger  $\text{CH}_3\text{NH}_2$  molecule gives not only a larger volume per anion compared to  $\text{NH}_3$  ( $779$  vs  $760 \text{ \AA}^3$ ) but also an even more enhanced anisotropy, which will affect the extent of lifting of the degeneracy of the  $t_{1u}$  orbitals on the  $\text{C}_{60}^{3-}$  anion, associated with control of the metal–insulator transition.<sup>7</sup> A satisfactory crystal-chemical understanding of how this is achieved requires the determination of the location of the extra methyl group.

Analysis of the diffraction dataset with Rietveld refinement and difference Fourier map techniques was therefore initiated with the structural model<sup>6</sup> of  $(\text{NH}_3)\text{K}_3\text{C}_{60}$  in which the pseudo-octahedral  $\text{K}^+$  is displaced from the site center  $(\frac{1}{2}, 0, 0)$  by a displacement vector  $(\delta x, -\delta x, 0)$ , while the ammonia molecule resides along the  $[110]$  basal plane diagonal in the opposite direction to  $\text{K}^+$ . However, the resulting fit was unsatisfactory. The search for the location of the intercalated  $\text{CH}_3\text{NH}_2$  is challenging, given the weak X-ray scattering power of the light elements and the considerable structural disorder. Therefore, we treated the  $\text{K}^+ - \text{N} - \text{C}$  unit as a rigid body ( $\text{K}^+ - \text{N}$  and  $\text{N} - \text{C}$  bond lengths =  $2.54$  and  $1.479 \text{ \AA}$ , respectively,  $\text{K}^+ - \text{N} - \text{C}$  angle =  $109.46^\circ$ ) and performed a search of its location by allowing it to move rigidly along the  $[110]$  basal plane diagonal and monitoring the resulting quality-of-fit factors ( $R_{wp}$ ) of the Rietveld refinements until a single deep minimum was identified. This was followed by successive series of refinements where the  $\text{K}^+ - \text{N} - \text{C}$  unit was allowed translational freedom in the  $ab$  plane, the  $\text{CH}_3$  group was rotated about the  $\text{K}^+ - \text{N}$  bond, and the positional parameters and occupation numbers of the  $\text{K}^+ - \text{N} - \text{C}$  units were

<sup>†</sup> University of Liverpool.

<sup>‡</sup> University of Durham.

<sup>§</sup> University of Edinburgh.

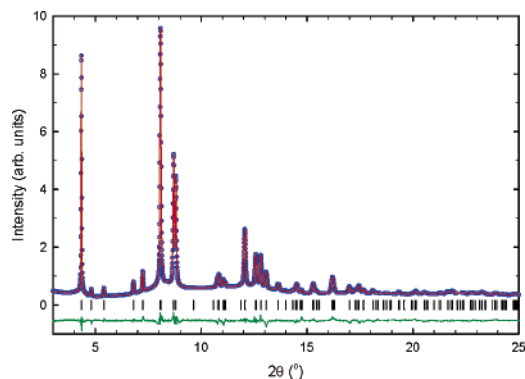


**Figure 2.** Final observed (○) and calculated (—) synchrotron X-ray diffraction profile ( $\lambda = 0.63782$  Å) for  $(\text{CH}_3\text{NH}_2)\text{K}_3\text{C}_{60}$  at 295 K ( $a = 15.2027(8)$  Å,  $b = 15.1800(9)$  Å,  $c = 13.5032(3)$  Å, space group  $Fm\bar{3}m$ , agreement factors of the Rietveld refinement:  $R_{\text{wp}} = 4.34\%$ ,  $R_{\text{exp}} = 1.64\%$ ). The lower solid line shows the difference profile, and the tick marks show the reflection positions.

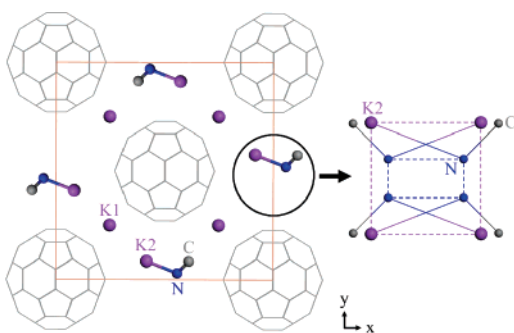


**Figure 3.** Basal-plane projection of the structure of  $(\text{CH}_3\text{NH}_2)\text{K}_3\text{C}_{60}$  at ambient temperature with one complex ion orientation per octahedral site shown. The four  $\text{K}^+-\text{N}-\text{C}$  units ( $\text{K}^+-\text{N} = 2.31(2)$  Å,  $\text{N}-\text{C} = 1.479$  Å,  $\text{K}^+-\text{N}-\text{C} = 108.0(3)^\circ$ ), which are disordered over the corners of two interpenetrating rectangles per octahedral site are shown at the right-hand side. The tetrahedral site  $\text{K}^+$  ions are not coordinated to  $\text{CH}_3\text{NH}_2$ .

refined. The results of the final Rietveld refinements are shown in Figure 2 with the fitted parameters summarized in Table 1S and the refined structure shown in projection in Figure 3. Refinement of the fractional occupancy of the  $\text{K}^+-\text{N}-\text{C}$  ion resulted in a nominal stoichiometry of  $(\text{CH}_3\text{NH}_2)_{1.06(1)}\text{K}_3\text{C}_{60}$ .

The  $\text{K}^+-\text{NH}_2-\text{CH}_3$  units occupy the octahedral sites with  $\text{K}^+$  and N disordered over the corners of two concentric rectangles. Examination of the fullerene–H–C contacts reveals shortest distances of 2.25–2.32 Å. Therefore, incorporation of  $\text{CH}_3\text{NH}_2$  into the  $\text{K}_3\text{C}_{60}$  sublattice leads to three important effects: (i) the lattice expands drastically by  $\sim 7\%$ , comparable to what has been achieved before for  $(\text{NH}_3)\text{Rb}_3\text{C}_{60}$ ,<sup>1</sup> (ii) the expansion is significantly anisotropic ( $\text{C}_{60}-\text{C}_{60}$  long/short contact = 1.057 vs 1.052 in  $(\text{NH}_3)\text{Rb}_3\text{C}_{60}$ ),<sup>1</sup> and (iii) the introduction of fullerene–H–C interactions. All these should have a profound effect on the electronic properties of the fulleride phases as they control sensitively the width,  $W$  of the  $t_{1u}$ -derived band and the critical value of the  $(U/W)$  ratio promoting the occurrence of a Mott–Hubbard transition driven by the on-anion interelectron repulsion  $U$  to an antiferromagnetic insulating state.<sup>1,7</sup> Therefore, we measured the temperature dependence of the total magnetic susceptibility,  $\chi$ , of  $(\text{CH}_3\text{NH}_2)\text{K}_3\text{C}_{60}$  which was obtained from the difference of the values measured at

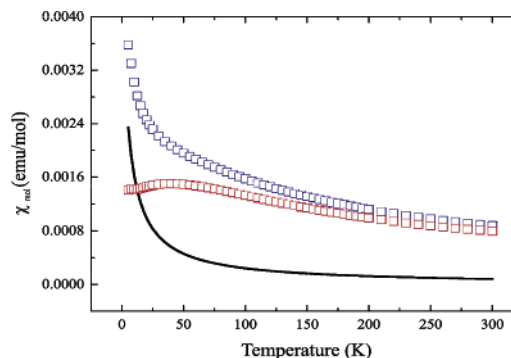


**Figure 4.** Temperature dependence of the magnetic susceptibility,  $\chi$  (red squares) of  $(\text{CH}_3\text{NH}_2)\text{K}_3\text{C}_{60}$  following subtraction of the Curie tail (solid line), attributable to paramagnetic impurities, from the total measured susceptibility (blue squares).

5 and 2 T in order to remove the influence of ferromagnetic impurities (Figure 4). Its value at 300 K is  $8.8 \times 10^{-4}$  emu mol<sup>-1</sup>, comparable to those of  $\text{K}_3\text{C}_{60}$  and  $(\text{NH}_3)\text{K}_3\text{C}_{60}$ . Between 300 and 100 K,  $\chi$  follows the Curie–Weiss law, yielding an effective moment of  $1.78(8) \mu_{\text{B}}/\text{C}_{60}$  (corresponding to  $S = 1/2$ ) with a Weiss temperature of  $-151(1)$  K. Due to the presence of a significant Curie tail at low temperatures, corresponding to a small paramagnetic impurity due to lattice defects, the raw data do not readily reveal the magnetic behavior at lower temperatures. However, if, in analogy with the ammoniated analogues,<sup>1</sup> a Curie–Weiss impurity term (6.8%) with  $S = 1/2$  and  $\theta = 5.8$  K is subtracted, a weakly temperature-dependent term is revealed, showing a broad maximum in  $\chi(T)$  in the vicinity of 40–50 K that may be associated with the onset of a transition to a long-range ordered antiferromagnetic state.

The demonstration that methylamine can be incorporated into fulleride lattices opens up the possibility of exploiting fullerene–H–C interactions to control structures in which fulleride frontier orbital degeneracy is utilized to give metallic, insulating and superconducting properties. It is significant that larger units than ammonia can be inserted to coordinate to the metal cations while retaining a structure related to close-packing and with significant electronic interactions between the fulleride anions

**Acknowledgment.** We thank the EPSRC for financial support (K.P., M.J.R.), the ESRF for provision of beamtime, and Dr. A. N. Fitch (ESRF) for help with the experiments.

**Supporting Information Available:** Additional experimental details, MAS <sup>1</sup>H NMR spectrum of  $(\text{CH}_3\text{NH}_2)\text{K}_3\text{C}_{60}$ , structural parameters from the Rietveld refinement. This material is available free of charge via the Internet at <http://pubs.acs.org>.

## References

- (1) Margadonna, S.; Iwasa, Y.; Takenobu, T.; Prassides, K. *Struct. Bonding* **2004**, *109*, 127–164.
- (2) Cooke, S.; Glenis, S.; Chen, X.; Lin, C. L.; Labes, M. M. *J. Mater. Chem.* **1996**, *6*, 1–3.
- (3) Highly crystalline material can be also prepared by dissolving stoichiometric amounts of  $\text{K}_6\text{C}_{60}$  and  $\text{C}_{60}$  in liquid methylamine at  $-65$  °C under stirring for 2 h and removing excess methylamine by evacuation.
- (4) Winter, J.; Kuzmany, H. *Solid State Commun.* **1992**, *84*, 935–938.
- (5) Han, A. J.; Guo, J. G.; Yu, H.; Zeng, Y.; Huang, Y. F.; He, H. Y.; Long, Y. C. *ChemPhysChem* **2006**, *7*, 607–613.
- (6) Rosseinsky, M. J.; Murphy, D. W.; Fleming, R. M.; Zhou, O. *Nature* **1993**, *364*, 425–427.
- (7) Gunnarsson, O. *Alkali-Doped Fullerenes*; World Scientific: Singapore, 2004.

JA066295J